Impact of the shear strength reduction of a soil - geogrid interface to the stability of an embankment

J. Stacho[1] M. Sulovska[2]
Department of Geotechnics, Faculty of Civil Engineering, STU Bratislava, Slovakia,
jakub.stacho@stuba.sk[1], monika.sulovska@stuba.sk[2]

ABSTRACT: The paper deals with numerical analysis of the stability of an embankment reinforced using a geogrid. The reinforcement was a biaxial geogrid made of polypropylene with a tensile strength of a 30 $kN.m^{-1}$. The analysis is focused on modeling of an interface between geogrid and soils. The properties of the interface were measured using a modification of a large scale direct shear test apparatus. The tests showed a reduction of shear strength properties of the original soils of about 10 - 15 %. The numerical analysis takes into account three different types of soils for the construction of the embankment. The measurements showed that the impact of the shear strength reduction on the interface between geogrid and soils increases with decreasing grain sizes. The results of the analysis showed that the modeling of the interface between geogrid and soils has a significant impact on horizontal deformations, bulging of the embankment, as well as the settlement of the embankment.

Keywords: reinforced soil; geogrid; properties of interface; embankment; numerical modeling

1. Introduction

Mechanically Stabilized Earth Walls and Reinforced Soil Slopes are cost-effective structures that use tensile reinforcing synthetics elements in the soil. These elements, such as e.g., geogrids and geotextiles, increase the strength and stability of the earth's construction. Advantages and possibilities of their use were published by [1]. The geosynthetics can be used for the design of reinforced embankments to improve the main body of the embankment or to improve the subsoil and base of the embankment, e.g., [2 – 4]. The use of geosynthetics for the design of reinforced embankments of reinforced earth walls in the region of Slovakia was published by, e.g., [5]. Numerical analysis of soil structures improved using geogrid was presented by, e.g., [6] [7] [8]. Geng, et al. [6] presented numerical analysis which showed that the use of geogrid improves the redistribution of stresses in a reinforced embankment and reduces the effect of the non-uniform settlement. Majedi, et al. [7] presented a parametric study focused to impact of embankment slope and number of geogrid layers to stability and deformation of the embankment. They stated that the use of geogrid cause a decrease in horizontal deformation of the embankment and lead to an increase in safety factor.

The design of these constructions using numerical modeling or analytical approach requires properties of soils, geogrids as well as properties of an interface between soil and a geogrid. The determination of soil-geogrid interface properties is a separate problema, which were analyzed by many researchers, e.g., [9] [10] [11]. Properties of a soil-geogrid interface are usually given by a reduction coefficient α which represents the ratio of shear strength of soil-geogrid interface and pure unreinforced soil. The coefficient α determined using conventional methods is usually smaller than 1.0 and rarely exceeds 1.0. The results of measurements of soil-geogrid properties presented by authors [12] of the paper showed that the coefficient α for coarse-grained soils is within the range of 0.79 - 1.04. In the case of fine-grained soils, the coefficient α is within the range 0.7 - 0.9, presented also by technical approach TP79/2008 [13]. The paper presents a numerical analysis based on the parametric study focused on the modeling of the geogrid interface and its impact on the deformations and stability of the embankment. Two simple educational examples were selected. The first example was a model of the embankment with slopes and the second example was a model of a reinforced retaining wall made of concrete blocks. The study included two options when the main body of the embankment is made of coarse-grained soils and fine-grained soils.

2. Laboratory testing of the soil-geogrid interface

The properties of the soil-geogrid interface were measured using a large-size SHEARMATIC 27-WF 2304 direct shear test apparatus (Fig. 1). The shear box of the apparatus has dimensions of 300 x 300 mm and the height of 200 mm. The tests were fully automatized.

Figure 1. Large-size direct shear test apparatus

The tests were executed with samples of the weight of 28.0 kg. The samples were compacted with a rubber hammer to achieve the maximal possible density. In the case of a coarse-grained material, the samples were compacted to a density index I_d = 0.85. The normal stresses were selected at the values of 50, 100 and 150 kPa. The maximal horizontal movement was 60 mm. The tests were executed in two main steps. *The first step* was the execution of the tests for pure samples to obtain shear strength properties of unreinforced soil. In *the second step*, the geogrid was fixed to an upper immovable part of the shear box and the tests were repeated (detail of fixing the geogrid is shown in Fig. 2). It allowed determining the soil-geogrid interface shear strength properties. The reduction coefficient α was computed using Eq. (1):

$$\alpha = \frac{\tau_{soil-geogrid}}{\tau_{soil}} \tag{1}$$

where $\tau_{\text{soil-geogrid}}$ is the shear strength of soil-geogrid interface a τ_{soil} is the shear strength of pure unreinforced soil.

Figure 2. Fixing the geogrid to the upper part of the shear box

2.1. Parameters of the geogrid tested

The study presented in this article was based on the results of measurements using the Thrace TG3030S geogrid. It is a biaxial geogrid made of polypropylene (PP) using the extrusion method of punching a pattern of holes, which is followed by stretching under controlled temperature. The main properties of the geogrid are presented in Table 1.

Table 1. Properties of geogrid tested

Parameter (unit)	Value
Tensile strength - MD / CD ($kN.m^{-1}$)	30 / 30
Minimal tensile strength - MD / CD ($kN.m^{-1}$)	11 / 11
Mesh size - MD / CD (mm)	40 x 40
Grid opening space (%)	77.43

2.2. Results of the soil-geogrid interface testing

The results of the shear tests for the coarse-grained sample are presented in Fig. 3, which includes the failure envelope curves for peak and residual state of unreinforced and reinforced soil. The shear strength properties determined are presented also in Fig. 3, where φ' is the peak angle of shear strength, τ_0' is the peak initial shear strength, φ_r' is the residual angle of shear strength and $\tau_{0,r}'$ is the residual initial shear strength.

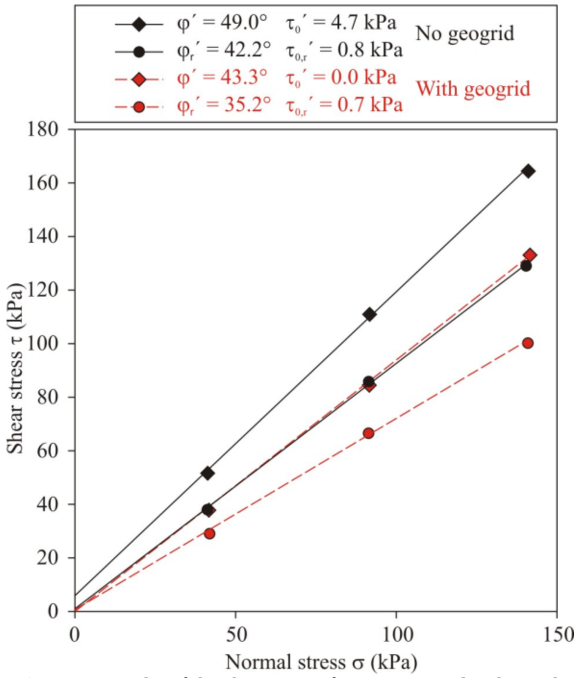

Figure 3. Results of the shear tests of coarse-grained soil sample

Using equation (1), the coefficient α was determined on the angle of the shear strength. The values of the coefficient α are given in Table 2. The initial shear strength τ_0' caused by the interlocking of grains was measured in a range of 0 - 4.7 kPa. This value was negligent for the parametric study. The coefficients α for fine-grained soil were determined the same way and their values are presented in Table 2.

Table 2. Coefficient α determined using laboratory testing

Soil		Coarse-grained	Fine-grained
Angle of shear strength	Peak	0.884	0.690
	Residual	0.835	0.911
	Average	0.859	0.801

3. Numerical model for parametric study

Numerical modeling based on the Finite Element Method (FEM) was done using the Plaxis 2D geotechnical software. The parametric study included two simple educational examples:

- *Model 1* - embankment with slopes;
- *Model 2* - embankment supported with reinforced retaining walls made of concrete blocks.

The part of the subsoil below the embankment was the same in both models. Because of the symmetry, only one side of the model was modeled. The dimensions of the subsoil were 40 x 20 m. The soils were modeled using the Hardening Soil material model [14]. The subsoil was homogeneous, the GWL (groundwater level) was taken into account 1.0 m below the surface. The parametric study included two cases when the body of the embankment is made of coarse-grained soil as well as fine-grained soil. The properties of all soils are presented in Table 3.

Table 3. Input properties of soils used in numerical modeling

Soil	Subsoil	Embankment	
Parameter (unit)		Coarse-grained	Fine-grained
γ (kN.m^{-3})	18.5	21.3	18.5
γ_{sat} (kN.m^{-3})	20.2	21.7	20.2
$E_{50} = E_{oed}$ (MN.m^{-3})	50	100	25
E_{ur} (MN.m^{-3})	150	300	75
m	0.7	0.5	0.7
φ'	30	49	25
c'	15	0	15

The model was created using 15-node triangular elements. A standard fixities were used. The standard fixity generates a full fixity at the base of the geometry (vertical and horizontal movement is impossible) and a roller conditions at vertical sides of the geometry (only horizontal movement is impossible). The scheme of *Model 1* is shown in Fig. 4 and the scheme of *Model 2* is shown in Fig. 5.

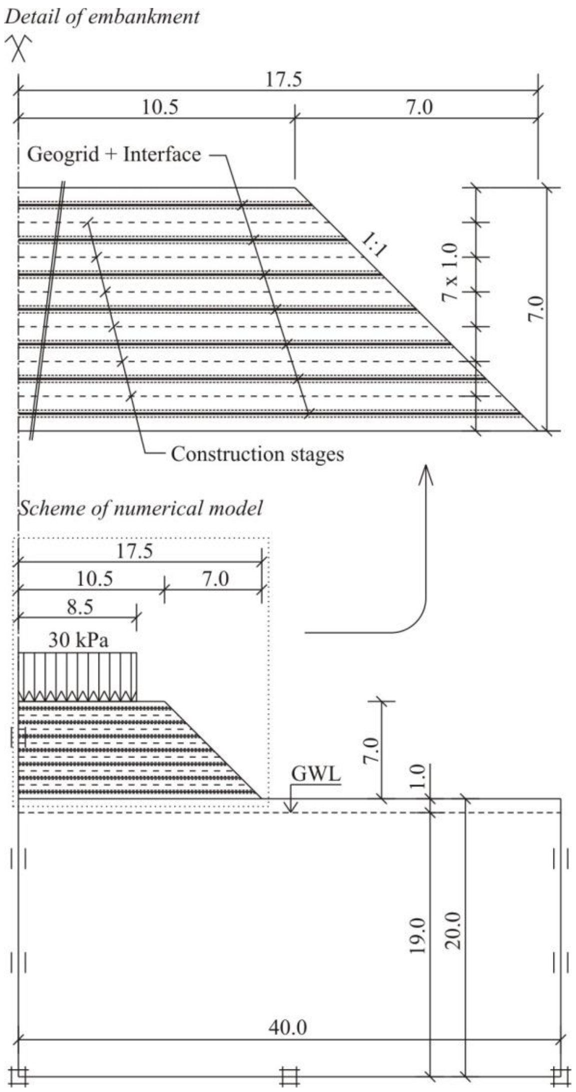

Figure 4. Scheme of *Model 1*

The embankment had a height of 7 m constructed in 7 layers with 7 geogrids in both cases. The top of the embankment had 10.5 m and a load of a 30 kPa acting in a length of 8.5 m from the axis. The differences of the model were sides of embankments and length of geogrids. Interfaces were modeled on both sides of geogrids. The interfaces were defined using parameter R_{inter} which represents the same value as the coefficient α. The value of the R_{inter} was variable and varied between 0.5 - 1.0 in the parametric study presented. The values measured using large-scale direct shear tests were included. In the case of *Model 2*, the geogrids were extended for 1 m with a constant value of the R_{inter} at the value of 1.0.

The numerical model has followed phases: initial phase for modeling of a initial stress state; modeling of a 0.5 height part of embankment (phase modeled as a consolidation phase); installation of geogrid (phase modeled as a plastic phase); next part of embankment of a height of 1 m (consolidation phase) and installation of next layer of geogrid. The whole embankment was modeled gradually this way. After the embankment was modeled to the total height, the distributed load of 30 kPa was activated. The last phase was the safety analysis which allowed determination of safety factor.

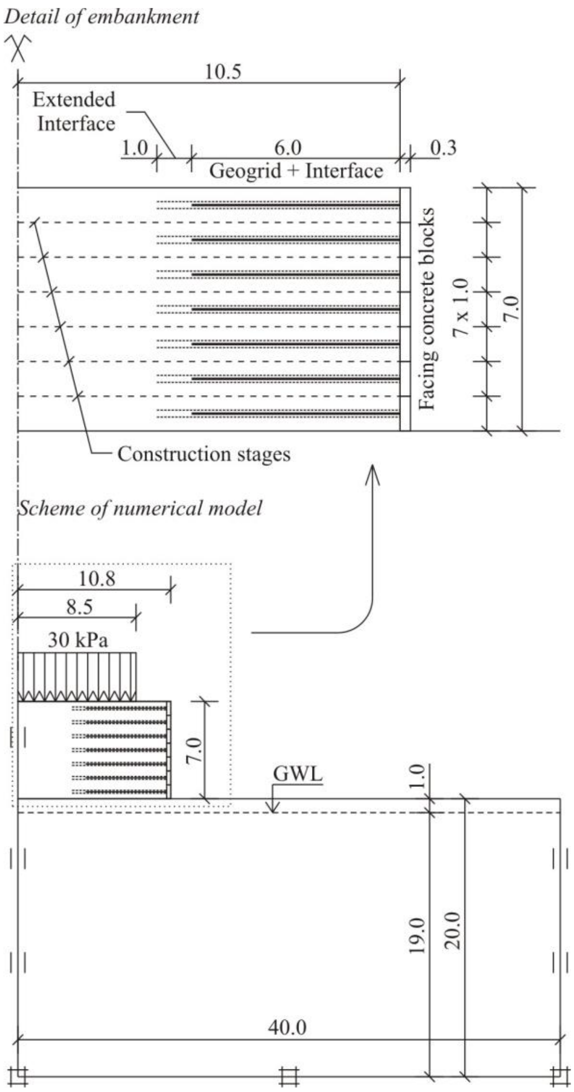

Figure 5. Scheme of *Model 2*

The coarseness of the mesh of the embankment is shown in the detail in Fig. 6 for *Model 1* and Fig. 7 for *Model 2*.

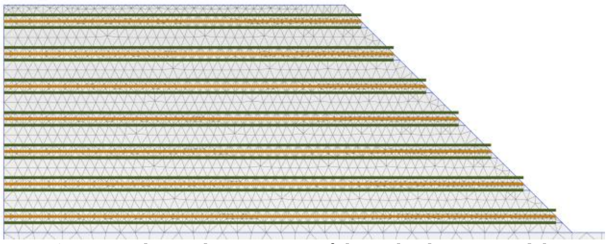

Figure 6. The mesh coarseness of the embankment, *Model 1*

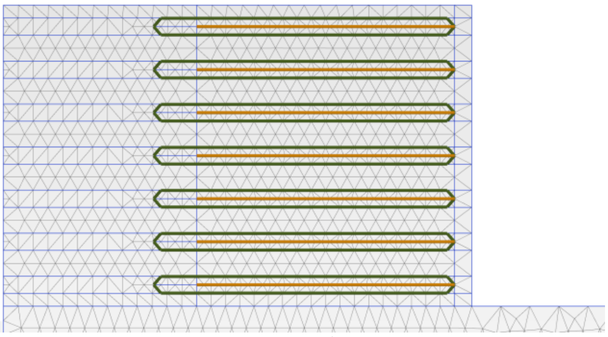

Figure 7. The mesh coarseness of the embankment, *Model 2*

4. Results of the parametric study and discussion

The results of numerical modeling of the *Model 1*, embankment with slopes, made of coarse-grained material are shown in Fig. 8 and Fig. 9. The parametric study is focusing on the impact of parameter R_{inter} on deformations and safety factors. The R_{inter} parameter varies in a range of 0.5 - 1.0. The results of laboratory tests showed that the value of R_{inter} is equal to 0.86 for geogrid used for the analysis presented – these results are highlighted with red curves. Vertical deformation of the top of the embankment is shown in Fig. 8. The change of the R_{inter} parameter has an impact only on vertical deformation of the side of the embankment which corresponding to horizontal deformation of the side of the embankment which is significantly affected by the change of the R_{inter} parameter. The difference in deformation between R_{inter} = 1 and R_{inter} = 0.86 values used are about 1 mm for vertical deformation and 2 mm for horizontal deformation. The reduction which was higher than 0.7 caused significantly bigger deformations for both directions.

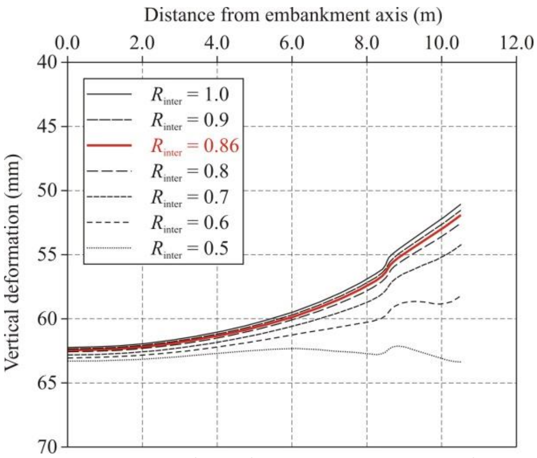

Figure 8. Settlement of top of the embankment made of coarse-grained soil, *Model 1*

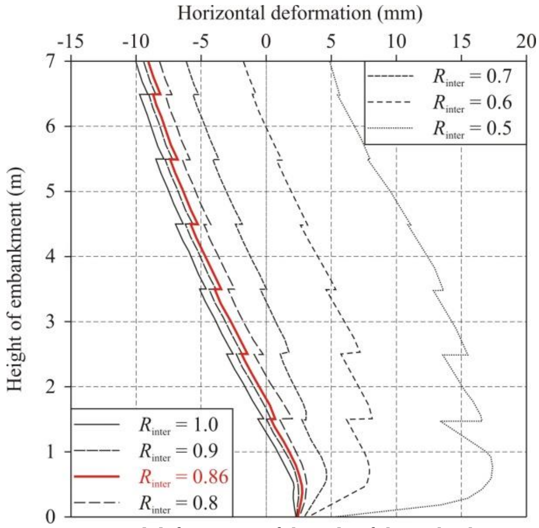

Figure 9. Horizontal deformation of the side of the embankment made of coarse-grained soi, *Model 1*

The detail of the deformed model of the embankment is shown in Fig. 10. The horizontal deformations, which are the most affected by using the geogrids, are shown in Fig. 11. In the case of the *Model 1* made of fine-grained soil, the R_{inter} was varied only between 0.6 to 1.0, the value represent the measurement was R_{inter} = 0.80. The change of the R_{inter} value has a significantly higher impact on the vertical deformation of the top of the embankment (Fig. 12) which was caused by also significantly higher deformation of the side of the embankment (Fig. 13). The shape of the deformations is affected also by cohesion and higher deformations were obtained because of smaller deformation parameters. The change of the R_{inter} parameter has only small impact on the vertical deformation of the middle of the embankment.

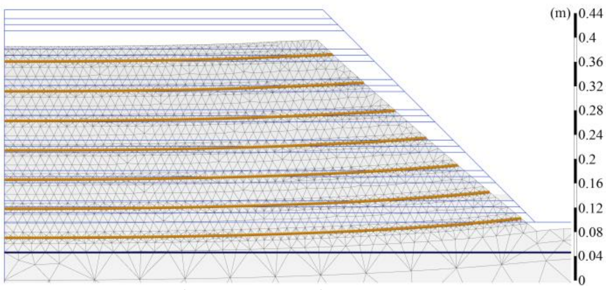

Figure 10. Deformed model of the embankment, *Model 1* (R_{inter} = 0.86)

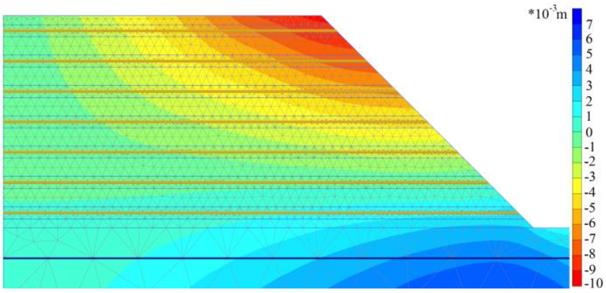

Figure 11. Horizontal deformations of the embankment, *Model 1* (R_{inter} = 0.86)

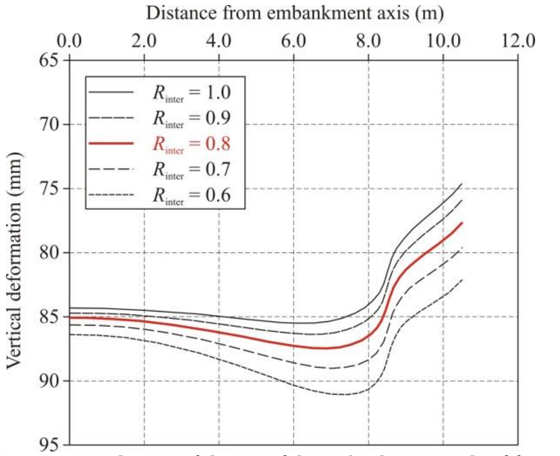

Figure 12. Settlement of the top of the embankment made of fine-grained soil, *Model 1*

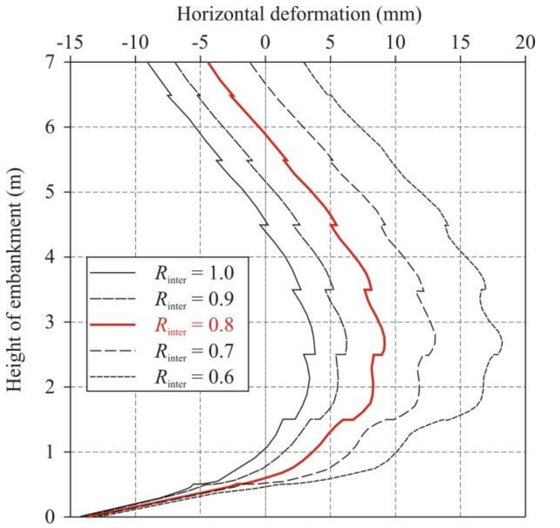

Figure 13. Horizontal deformation of the side of the embankment made of fine-grained soil, *Model 1*

The results of the numerical modeling of the *Model 2*, embankment supported using a reinforced retaining wall, made of coarse-grained soil are presented in Fig. 14 and Fig. 15. The significant change of vertical deformation of the top of the embankment is at the side (Fig. 14), where the reduction of R_{inter} parameter from 1.0 to 0.86 causing increasing of the vertical deformation for about 8 mm – near the side of the embankment, where the maximal deformation was achieved. In comparison to *Model 1*, *Model 2* has stiff sides which cause the different shape of horizontal deformation. At the bottom of the side, the impact of the R_{inter} can be negligent. The biggest horizontal deformation is achieved at the top of the side (top of the reinforced retaining wall). Change of the R_{inter} from 1.0 to 0.5 causes increasing of horizontal deformation from 24 mm to 64 mm. The use of the measured value of the R_{inter} causes horizontal deformation equal to 32 mm. The detail of the deformed model of the embankment is shown in Fig. 16. The horizontal deformations mostly affected by using the geogrids are shown in Fig. 17.

The similar results were obtained also in case of the embankment made of fine-grained soils. The values of deformations are bigger because of the properties of fine-grained material of the embankment. The results of the vertical deformations of the top of the embankment are shown in Fig. 18 and horizontal deformations of the side are shown in Fig. 19.

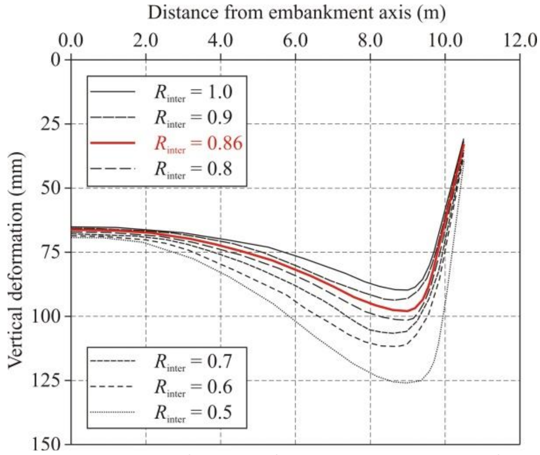

Figure 14. Settlement of the top of the embankment made of coarse-grained soil, *Model 2*

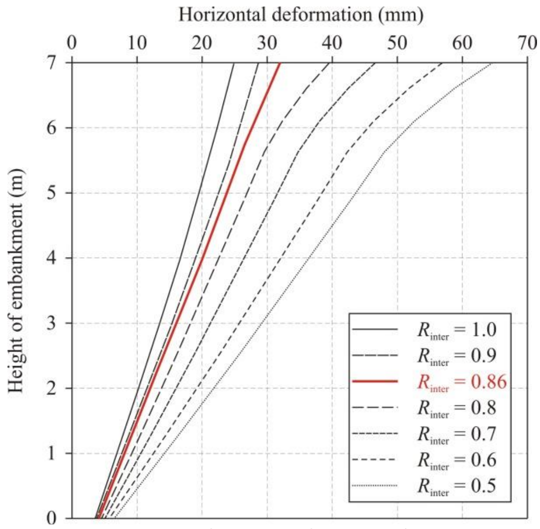

Figure 15. Horizontal deformation of the side of the embankment made of coarse-grained soil, *Model 2*

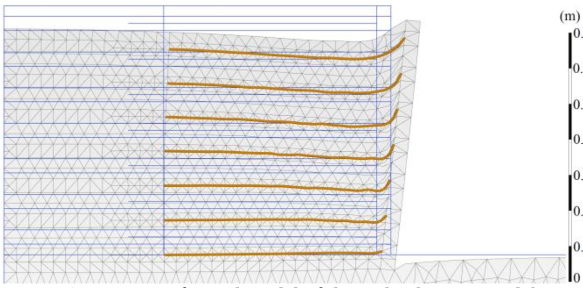

Figure 16. Deformed model of the embankment, *Model 2* ($R_{inter} = 0.8$)

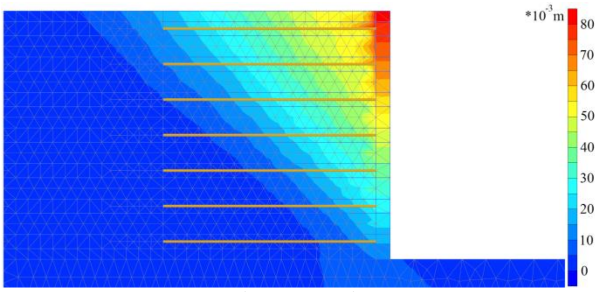

Figure 17. Horizontal deformations of the embankment, *Model 2* ($R_{inter} = 0.8$)

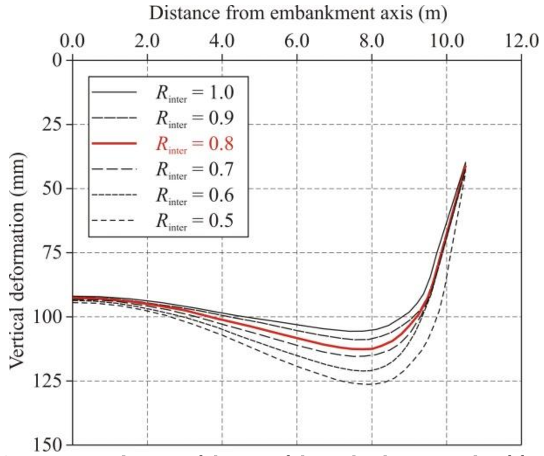

Figure 18. Settlement of the top of the embankment made of fine-grained soil, *Model 2*

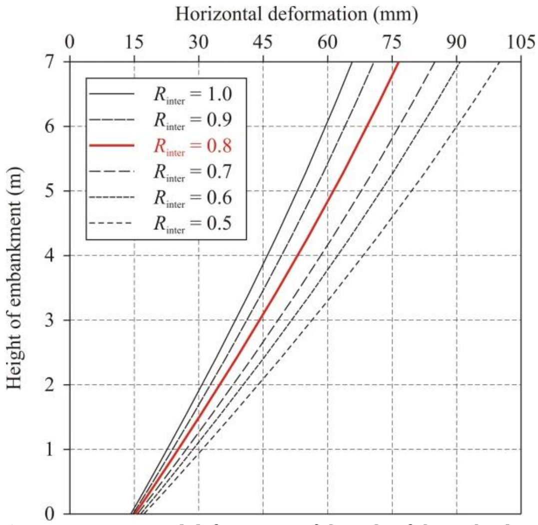

Figure 19. Horizontal deformation of the side of the embankment made of fine-grained soil, *Model 2*

In addition to deformations, an impact of R_{inter} parameter change to the safety factor was analyzed. The results of the safety factor obtained for embankments made of coarse-grained soil for both models are shown in Fig. 20.

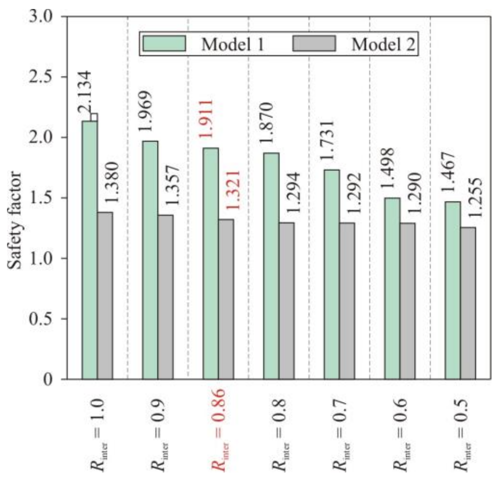

Figure 20. Safety factor for embankments made of coarse-grained soil

The change of the value of the R_{inter} parameter has a significantly higher impact in the case of the *Model 1*, where the safety factor decrease from 2.134 (R_{inter} = 1.0) to 1.467 (R_{inter} = 0.5). In the case of R_{inter} = 0.86, the value of safety factor 1.911 was obtained. In the case of *Model 2*, the impact of the change of the value of the R_{inter} parameter on the safety factor is very small. The similar results were obtained also in the case when the embankments for both models are made of fine-grained soils (Fig. 21).

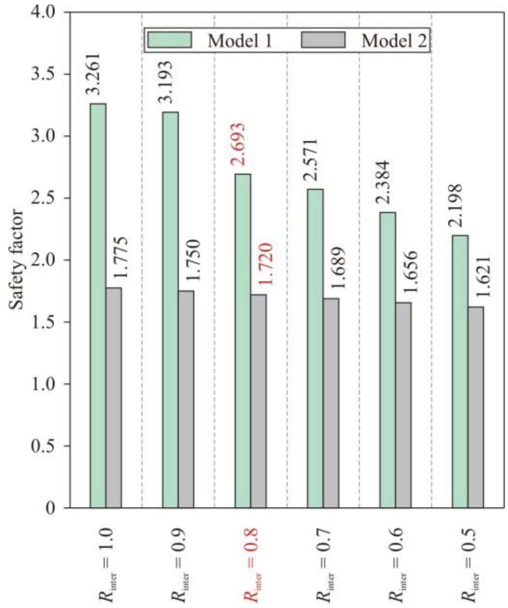

Figure 21. Safety factor for embankments made of fine-grained soil

The change of the value of the R_{inter} parameter has a significantly bigger impact on the safety factor in *Model 1* than in *Model 2*.

5. Conclusion

Design of the reinforced earth structure using analytical computational models or numerical modeling, FEM, requires the definition of soil-geogrid interface properties. The interface is usually defined with a parameter, marked R_{inter} in this article, which represents the reduction of shear strength properties on the contact between soil and geogrid. The results of a parametric study focused on the impact of the R_{inter} parameter to deformations and safety factors are presented. Simple models, the model of the embankment with slopes and model of embankment supported using reinforced retaining walls, were used for the study. The analysis includes two cases when the embankments are made of coarse-grained soil and fine-grained soils. The properties of the soil-geogrid interface were measured using large-scale direct shear test apparatus. Based on the results of the tests, the R_{inter} parameter at the value of 0.86 for coarse-grained soil and at the value of 0.80 for fine-grained soil was used.

The results of the parametric study in the case of the Model 1 showed that the change of the value of the R_{inter} parameter affected horizontal deformation of the side of the embankment as well as the vertical settlement of the side of the top of the embankment. The differences between R_{inter} = 1.0 and a measured R_{inter} were significantly higher in the case of the embankment made of fine-grained soil. In the case of Model 2, the change of the R_{inter} = 1.0 to the measured R_{inter} caused increasing of horizontal deformation of the embankment of about 22 % in the case of the embankment made of coarse-grained soil and about 16 % in the case of fine-grained soil. The change of the R_{inter} value has an impact also on the safety factor when its impact was significantly higher in the case of *Model 1* than in *Model 2*.

The value of R_{inter} used for the design of any reinforced soil structure has an impact on its deformations and stability and because of this, the correct value of the R_{inter} should be used. One of the most appropriate methods of determining the soil-geogrid interface properties is a large-scale direct shear test. The article includes two simple examples, but it can be assumed, that the impact of the change of the R_{inter} parameter will be much bigger in case of complex difficult reinforced soil structures.

Acknowledgement

The project presented in this article is supported by the VEGA Grant No. 1/0530/19.

References

[1] Ryan R., Berg, P. E., Barry R., Christopher, P. E., Naresh C., Samtani, P. E. "Design and Construction of Mechanically Stabilized Earth Walls and Reinforced Soil Slopes – Volume I", U. S. Department of Transportation Publication Federal Highway Administration, Washington, D. C., United States, Rep. FHWA-NHI-10-024, 2009, Available at: https://www.fhwa.dot.gov/engineering/geotech/pubs/nhi10024/ [Accessed: 20, 08, 2019].

[2] Blackwood, T. W., Vulova, C. V. "Geogrid reinforced embankment constructed over peat soil in clark country", In: Airfield and Highway Pavements Specialty Conference 2006, Atlanta, Georgia, United States, 2006, pp. 317-328. https://doi.org/10.1061/40838(191)27

[3] Meyer, R., Shao, Y. "Geogrid-Reinforced and Pile-Supported RoadWay Embankment", In: Geo-Frontiers Congress 2005, Austin, Texas, United States, 2005, pp. 13. https://doi.org/10.1061/40777(156)9

[4] Arulrajah, A., Abdullah, A., Bo, M. W., Bouazza, A. "Ground improvement techniques for railway embankments", Proceedings of the Institution of Civil Engineers: Geotechnical Engineering, 162(1), pp. 3-14, 2009. https://doi.org/10.1680/grim.2009.162.1.3

[5] Dolinajova, K., Snahnican, J. "Geogrid and Double Twist Steel Mesh Reinforced Soil Walls Subjected to High Loads in a Seismic Area", In: Proceedings of the 12th Slovak Geotechnical Conference, 55 Years of Geotechnical Engineering in Slovakia, Bratislava, Slovakia, 2015, pp. 79-87.

[6] Geng, M., Li, P., Li, J. "Numerical Analysis of a Geogrid-Reinforced High Embankment", In: Fifth International Conference on Transportation Engineering, Dailan, China, 2015, pp. 1074-1083. https://doi.org/10.1061/9780784479384.135

[7] Majedi, P., Ghalehjough, B. K., Akbulut, S., Çelik, S. "Effect of Reinforcement on stability and Settlement of Embankment: A Finite Element analysis of Different Kinds of Reinforcing and Construction Conditions" European Journal of Advances in Engineering and Technology, 4(10), pp. 759-764, 2017, [online] Available at: http://www.ejaet.com/PDF/4-10/EJAET-4-10-759-764.pdf [Accessed: 20, 08, 2019].

[8] Peng, F., Li, F., Tan, Y. "FEM simulation of deformation and strength characteristics in geogridreinforced sand retaining wall under the change of loading rate", In: Geo-Frontiers Congress 2011, Dallas, Texas, United States, pp. 3807-3817, 2011. https://doi.org/10.1061/41165(397)389

[9] Palmeira, E. M., Antunes, L. G. S. "Large scale tests on geosynthetic reinforced unpaved roads subjected to surface maintenance", Geotextiles and Geomembranes, 28(6), pp. 547-558, 2010. https://doi.org/10.1016/j.geotexmem.2010.03.002

[10] Liu, C. N., Ho, Y. H., Huang, J. W. "Large scale direct shear tests of soil/pet-yarn geogrid interfaces", Geotextiles and Geomembranes, 27(1), pp. 19-30, 2009. https://doi.org/10.1016/j.geotexmem.2008.03.002

[11] Lee, K. M., Manjunath, V. R., "Soil-geotextile interface friction by direct shear tests", Canadian Geotechnical Journal, 37 (1), pp. 238-252, 2000. https://doi.org/10.1139/t99-124

[12] Súľovská, M., Stacho, J., Slávik, I. "Measurement of a Shear Strength of a Soil Reinforced Using a Geogrid", Buildustry, 1/2019, pp. 18-21, 2019, Available at: http://www.briainvenia.sk/images/pdf/sk/Buildustry-1_2019.pdf [Accessed: 24, 08, 2019].

[13] Ministry of Transportation, Department of Infrastructure "TP97/2008: Geosynthetics in the ground embankment of roads", Prague, Czech republics, pp. 72, 2008.

[14] Plaxis Software "PLAXIS 2D CONNECT Edition V20 – Material Models Manual", [online] Available at: https://www.plaxis.com/support/manuals/plaxis-2d-manuals/ [Accessed: 02, 02, 2020].